CHAPTER 5

HEAT TRANSFER IN FLOW BOILING

5.1 Experimental Conditions and Procedure

In the present investigation, upward flow boiling through a vertical quartz tube has been investigated experimentally using pure water and nanofluids with different concentrations. The boiling experiments have been conducted by gradually increasing the heat input to the cartridge heater until flow oscillation occurs. The temperature readings from the thermocouples have been recorded at 1 s time intervals and the heat input was controlled manually through the variac (SERVOCON). When flow oscillation was observed, then the data acquisition was terminated and the power supply was discontinued. The experiments on flow boiling were carried out at atmospheric pressure. The effect of supplied heat flux (30-250 kW/m^2), mass flux (3-20 kg/m^2s), inlet subcooling (20, 40 and 60K) and particle volume fraction (0.001%, 0.005% and 0.01% v/v) on heat transfer characteristics have been investigated**.** The flow boiling experiments using water and dilute oxide based nanofluids (Al_2O_3/water, TiO_2/water and SiO_2/water) have been conducted and results have been analyzed.

5.2 Validation of experimental set up with pure water

In order to evaluate the accuracy of the experimental setup, a series of experiments were conducted with pure water before measuring the convective heat transfer coefficients of nanofluids. The results with the pure water served as the basis for comparison with the results of nanofluids. The measured Nusselt numbers were compared with the Nusselt numbers obtained from the Gnielinski equation [140] for the turbulent flow.

Gnielinski equation for turbulent flows:

$$\mathrm{Nu_{pred}} = \frac{{}^{\mathrm{f}}/_{2}(\mathrm{Re}-1000)\mathrm{Pr}}{1+12.7\left({}^{\mathrm{f}}/_{2}\right)^{1/2}\left(\mathrm{Pr}^{2/3}-1\right)} \tag{5.1}$$

The friction factor, f, in the above equation can be calculated as follows [18]

$$\mathrm{f} = (0.79\ln\mathrm{Re} - 1.64)^{-2} \tag{5.2}$$

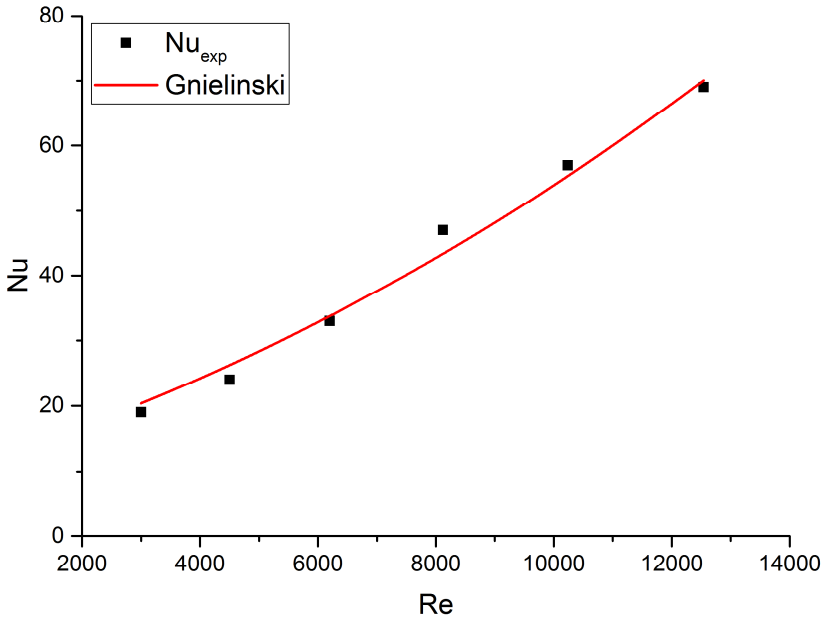

Fig. 5.1 Comparison between theoretical and experimental data for the Nusselt number of water

The Reynolds number of flow varied in the approximate range of 2,000 to 14,000. The Nusselt number obtained using correlations and by experimental data for pure water has been shown in Fig. 5.1. Reasonably good agreement can be seen between Gnielinski equation and the measurement over the Reynolds number range used in this study.

5.3 Boiling Curves

Boiling curves have been constructed for water and nanofluids using the wall temperatures measured at the thermocouple locations. Figure 5.2-5.5 show the boiling curves of water and different nanofluids at three different concentrations. The curves have been plotted at a fixed inlet subcooling of 20 K and mass flux of 12 kg/m^{2}s. The boiling curves show the classic trends of nucleate flow boiling. In the first part of these graphs, before the surface temperature reaches to the saturation temperature of fluid, both water and nanofluid have been heated by pure forced convection with the mechanism of single phase. There is almost a flat slope during the single phase heat transfer region. The heat transfer between the heat exchange surface and the fluid is almost similar during the forced convection stage. After entering the stage of nucleate boiling, the heat transfer capability is enhanced with the slope of the curves becoming larger. In this regime, the liquid near the wall is superheated and tends to evaporate, forming bubbles wherever there are active nucleation sites. The bubbles transport the latent heat of the phase change and also increase the convective heat transfer by agitating the liquid near the heating surface. The mechanism in this range is called nucleate boiling and is characterized by a very high heat transfer rate for only a small temperature difference.

As observed in the graphs, the boiling curves shift towards left for lower concentration of nanofluid compared to pure water, which indicates enhanced boiling performance. By adding nanoparticles to water, more power can be transferred from the heater surface to the surrounding fluid, resulting in a reduction of the wall superheat. However, with increasing concentration, boiling curve shifts towards right exhibiting deterioration in heat transfer. The shifted trend towards the right indicates that the heat transfers was decreased after further boiling in the nanofluid with higher concentration. Thus experiments suggest that heater surface is continuously modified morphologically

during nanofluid flow boiling, making nanofluid boiling performance dependent on applied heat flux and particle concentration. Nucleate boiling was the most crucial for the nanoparticle deposition on the heated surfaces. Higher heat flux leads to faster modification of the properties of the heater surface. The nanoparticle deposition on the heater caused by microlayer evaporation keeps modifying the heater surface and alter the boiling phenomenon. This phenomenon is predominant at higher concentration which causes delayed flow regime resulting from the wettability enhancement due to nanoparticle deposition.

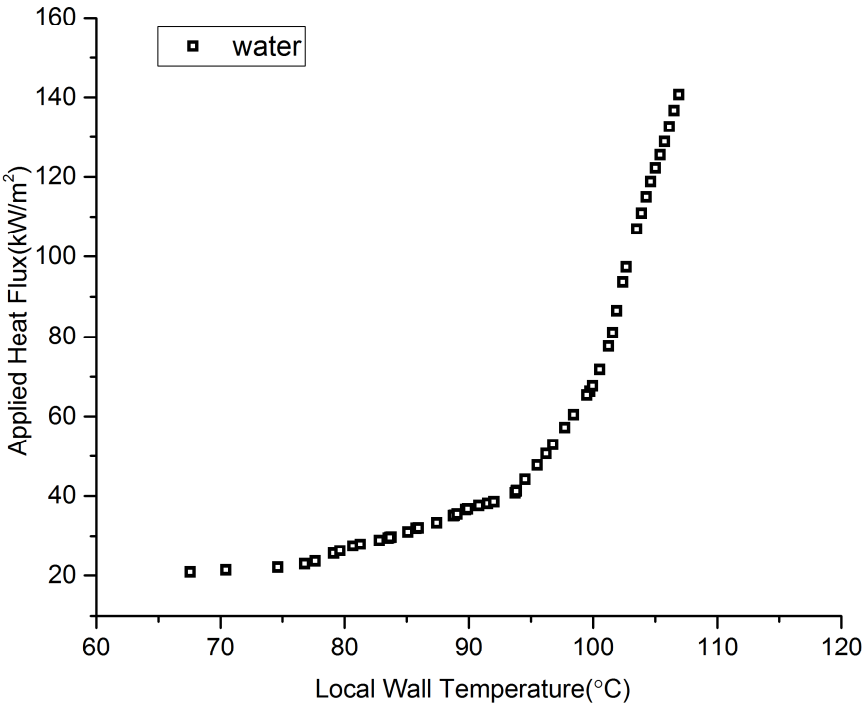

Fig. 5.2 Boiling curve of water (ΔT_{sub} = 20 K)

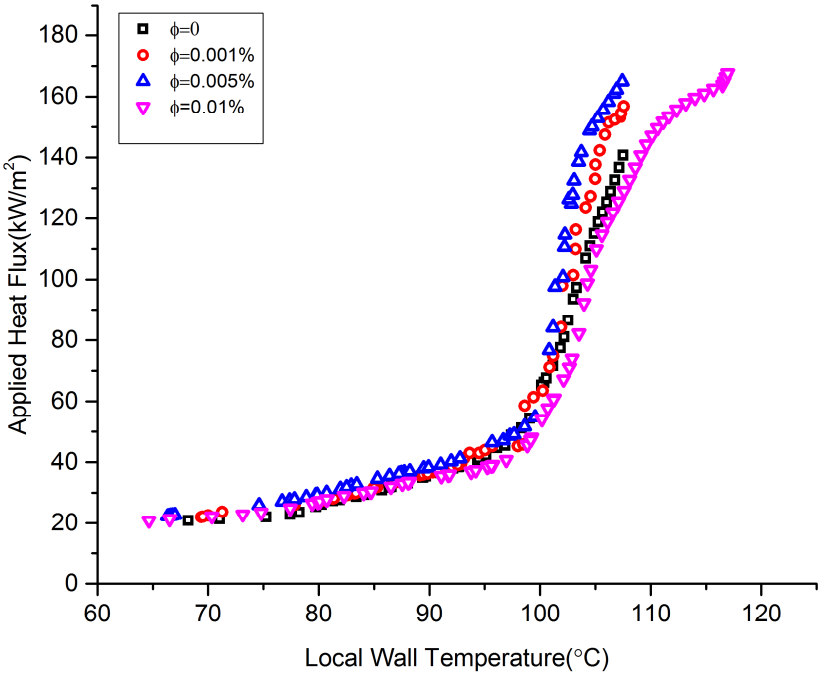

Fig. 5.3 Boiling curves of water and alumina nanofluid (ΔT_{sub} = 20 K)

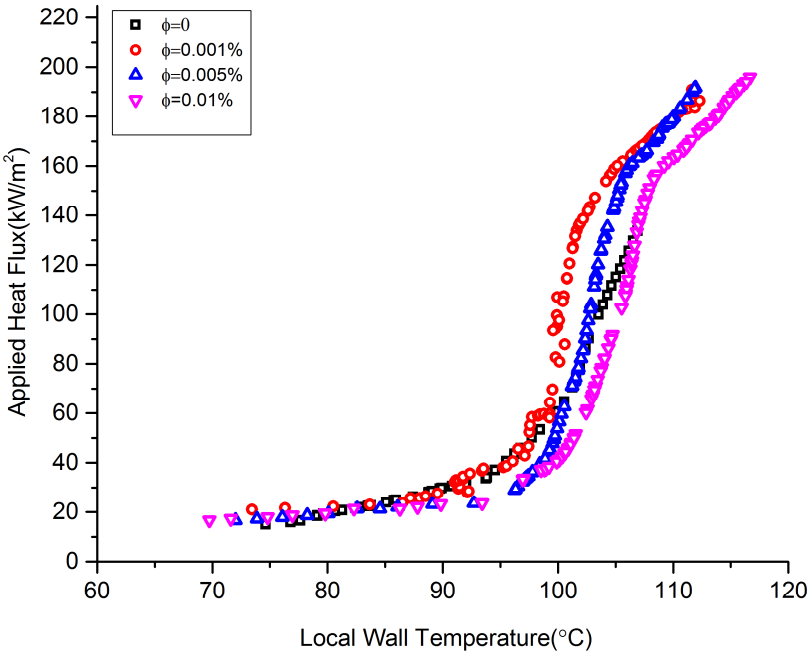

Fig. 5.4 Boiling curves of water and silica nanofluid (ΔT_{sub} = 20 K)

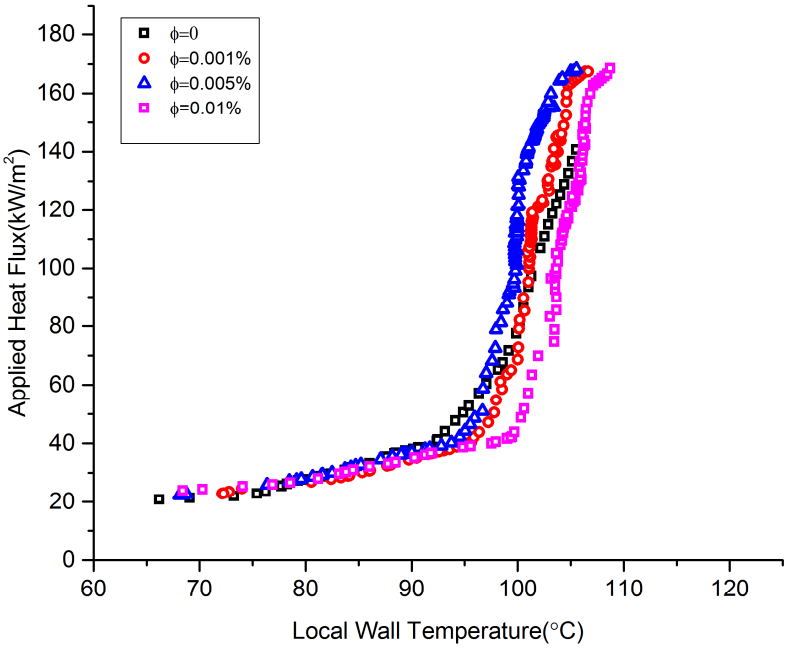

Fig. 5.5 Boiling curves of water and titania nanofluid (ΔT_{sub} = 20 K)

5.4 Heat Transfer coefficient

As the enhanced heat transfer performances of nucleate boiling of nanofluids are attributed to the deposition of nanoparticles, it is expected that the material and concentration of the nanoparticles may have significant effects on the nucleate boiling characteristics of nanofluids. In order to evaluate the effects of these parameters, further experiments have been conducted. It has been observed that the nanoparticles influence heat transfer mechanism in the convective zone. Also, they modify the dynamics of bubble nucleation by modifying surface properties. Both the aspects have contributed to the new augmenting features of nucleate boiling of nanofluids.

5.4.1 Effect of nanoparticle concentrations on heat transfer coefficient

The influence of heat flux on flow boiling heat transfer coefficient at a fixed mass flux of 12 kg/m^{2}s and fixed inlet subcooling of 20 K has been shown in Fig. 5.6-5.8. It

shows that for both water and nanofluids, heat transfer coefficient increases with increasing heat flux. However, in the convective region, heat transfer coefficient is drastically lower than that of nucleate boiling due to the sub-phenomena involved in nucleate boiling mechanism e.g. bubble formation. In fact, bubble transport is a considerable sub-phenomena comprising evaporation, micro/macro convection mechanisms induced by generated bubbles from the surface and subsequently condensing the bubbles inside the bulk of the liquid, which drastically enhance the heat transfer coefficient. Therefore, relatively higher heat transfer coefficient is obtained for nucleate boiling region. The porous layer formation due to nanoparticle deposition on the heater surface is an important characteristic in nucleate boiling of nanofluids. Evaporation of liquid microlayer causes deposition of nanoparticles which leads to increase in average nanoparticle concentration in the microlayer as compared to bulk liquid. Therefore, the nanoparticles in microlayer may play an important role in dissipating heat from the heater surface.

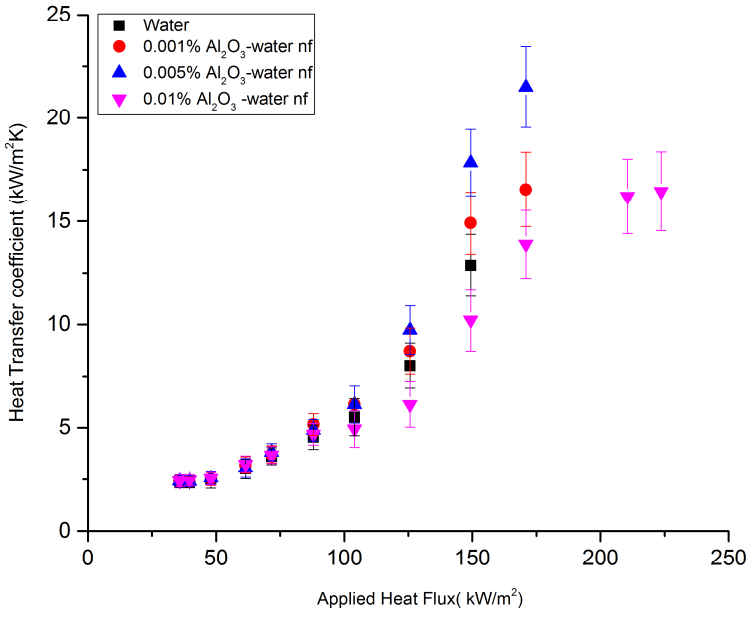

Fig. 5.6 HTC variation of alumina nanofluid

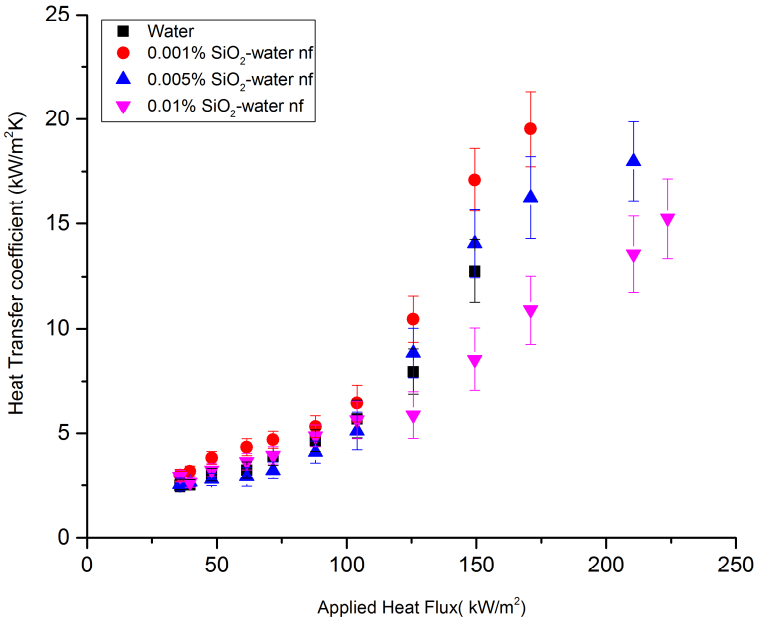

Fig. 5.7 HTC variation of silica nanofluid

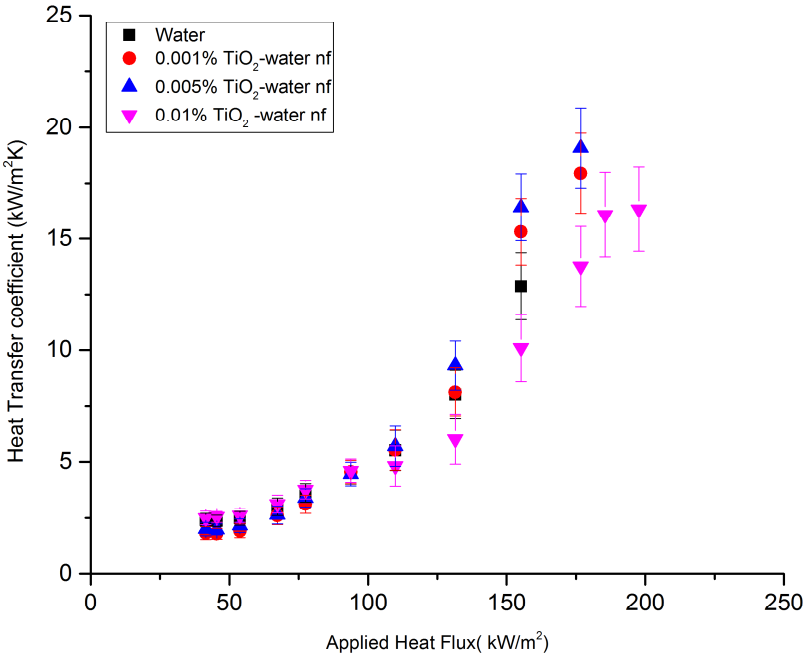

Fig. 5.8 HTC variation of titania nanofluid

Heat transfer coefficients (HTC) of water and nanofluids are almost similar at lower values of heat flux while the difference enhances at higher heat flux as observed in Fig. 5.6-5.8. During nucleate boiling, heat transfer rate is maximum, represented by higher slope in the graph. Nanoparticles cause fluctuations in the fluid and enhance energy exchange between the fluid and heater wall. It is observed that nanoparticles cause to enhance heat transfer in nanofluids as compared to pure water, however with increasing concentration, the heat transfer coefficient decreases. The factor responsible for such behavior of nanofluids is the increased thermal resistance caused by excess deposition of nanoparticles and interaction with nucleation sites on the heater wall at increased concentration during boiling. Such deposition is not uniform along the heater surface and can affect the micro cavities, thereby decreasing the heat transfer.

This could be interpreted in such a way that the surface modification has a significant influence on the heat transfer rate and that the HTC depends on heat flux density and the concentration of the nanofluids. Several possibilities could be associated with the reduction of the Boiling Heat Transfer (BHT) in case of higher concentration of nanofluid. The first possibility concerns the reduction of the number of nucleation sites which are affected by the excess deposition of nanoparticles. Related to this, the change in the size of the cavities which act as nucleation sites for the bubbles could also be another possible reason. Micro-sized cavities have been shown to be the ideal size for bubble nucleation. However, since the material deposited from the nanofluid is of nanometer size, it could be deposited onto the heater surface and the newly changed cavity after the deposition becomes smoother compared to the original rougher surface condition and possibly deactivates the nucleation site. SEM images of bare heater surface and nanoparticle deposited surface after experimentation with SiO_2-water nanofluid have been shown in Fig. 5.9.

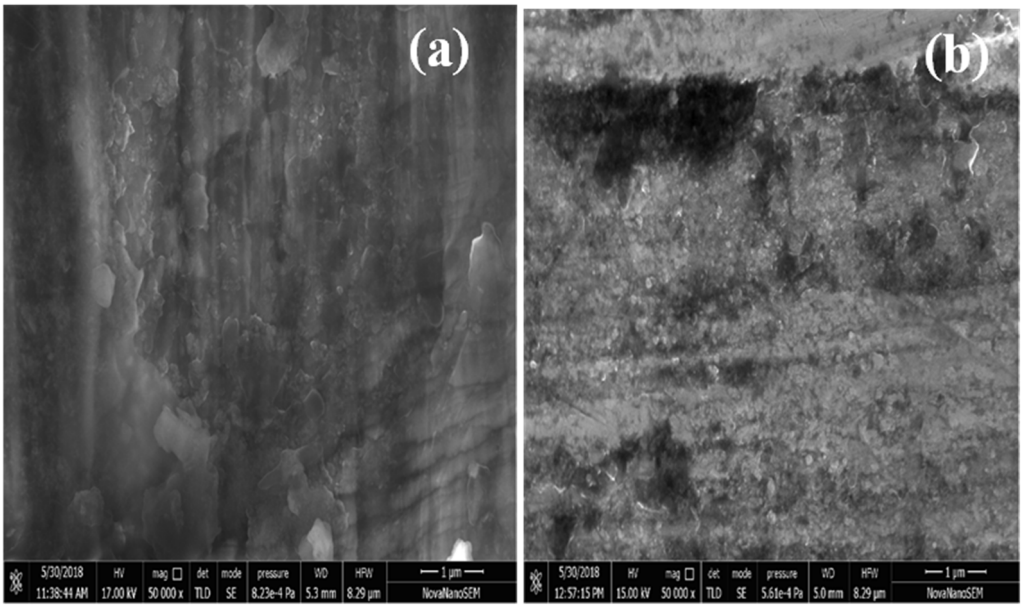

Fig. 5.9 SEM images of (a) bare heater surface

(b) nanoparticle deposited surface

Figure 5.6 compares the heat transfer coefficients of water to that of alumina nanofluid. It confirms that for 0.001 and 0.005 vol% concentration, the HTC increases as compared to the base fluid. However, for a concentration of 0.01vol%, the HTC deteriorates as compared to water. As clearly shown in the graph, the maximum enhancement of the heat transfer coefficient of alumina nanofluid occurs at 0.005% particle volume concentration and the enhancement is approximately 28% compared to water. For SiO_2/water nanofluid, the maximum enhancement is observed at 0.001% volume concentration and the enhancement is approximately 37.5% as compared to water. For TiO_2/water nanofluid, the maximum enhancement is observed at 0.005% volume concentration and the enhancement is approximately 20% as compared to water. These variations for different nanofluids are due to different type of nanoparticles present in the base fluid.

5.4.2 Effect of mass flux on heat transfer coefficient

The relationship of the heat transfer coefficient of water and three nanofluids (optimum concentration) with the mass flux has been shown in Fig. 5.10-5.13. The graphs have been plotted at a fixed inlet subcooling of 20K. As observed in the graph, no significant improvement in heat transfer coefficient is observed in single phase regime with increasing mass flux in water. Slightly higher values have been obtained only at mass flux of 20 kg/m^{2}s. With increasing heat flux, nucleate boiling begins earlier in case of 6.6 kg/m^{2}s as compared to 12, 17, 20 kg/m^{2}s (low mass fluxes as per the single pin reactor scaled down model) exhibiting higher heat transfer coefficient. However, the phenomenon is different in case of nanofluids. In the single-phase regime, an increase in mass flux results in a faster heat removal from the heater surface because of Brownian motion of nanoparticles. The increase in single phase heat transfer performance is attributed to nanoparticle interaction with the heater wall and working fluid. The effective conductivity of nanofluids increased by dispersion of suspended particles. However, the curves merge in the nucleate boiling regime, showing that the heat transfer is almost unaffected by the changes in the mass flux in case of nanofluids.

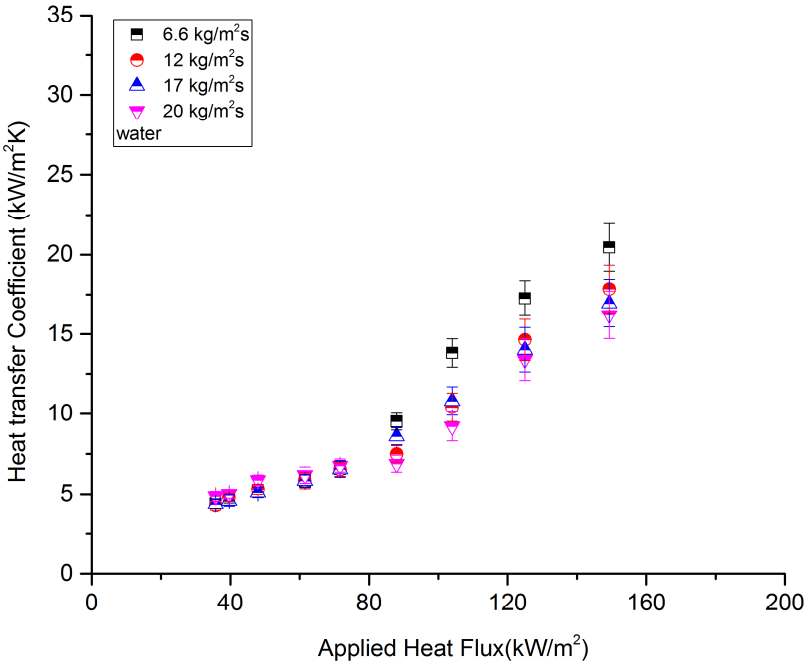

Fig. 5.10 Effect of mass flux on HTC of water

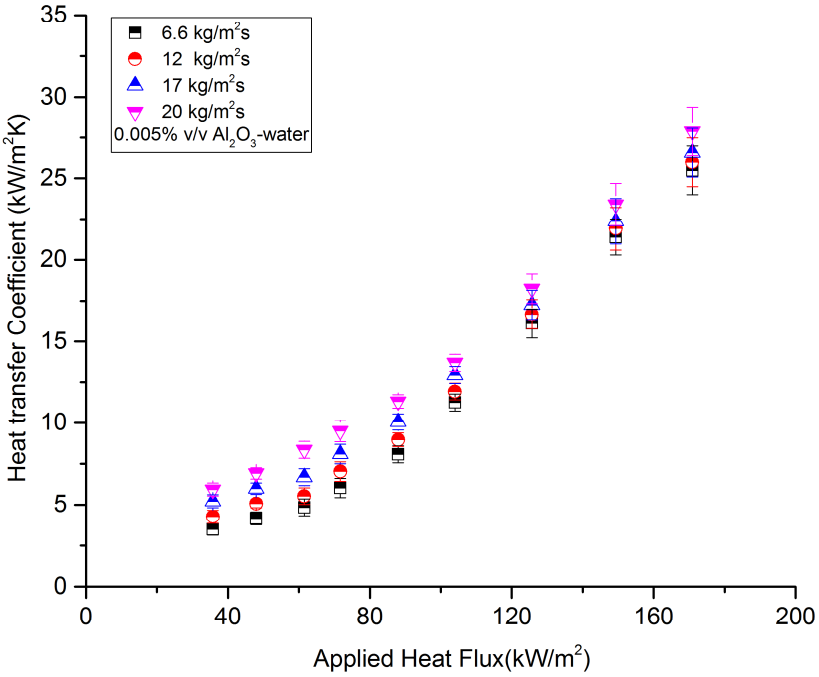

Fig. 5.11 Effect of mass flux on HTC of alumina nanofluid

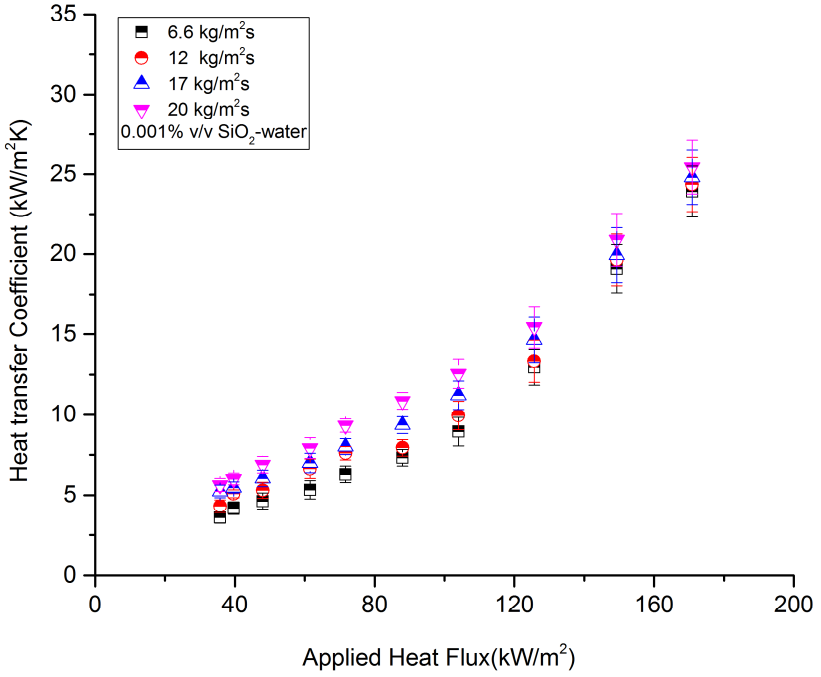

Fig. 5.12 Effect of mass flux on HTC of silica nanofluid

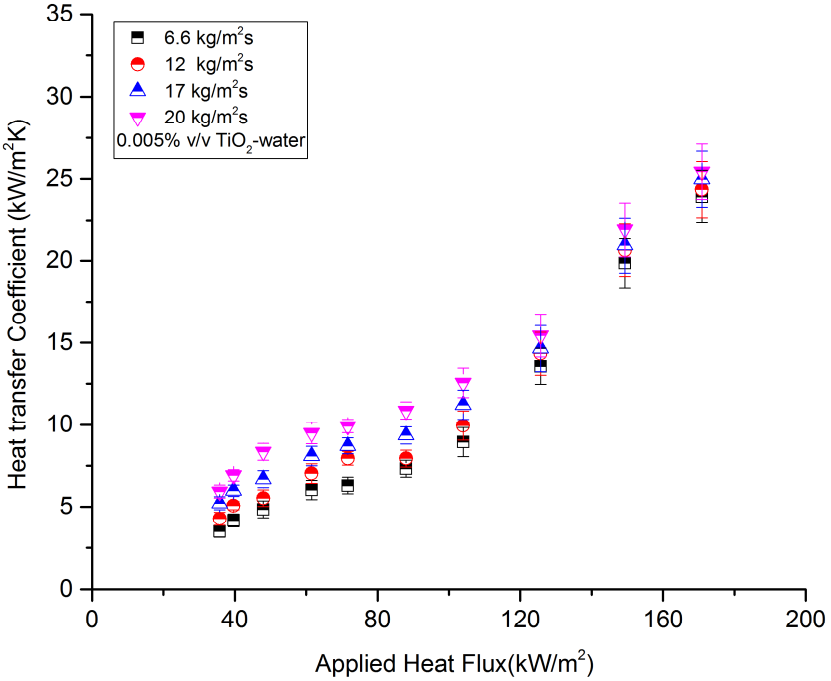

Fig. 5.13 Effect of mass flux on HTC of titania nanofluid

5.4.3 Effect of inlet subcooling on heat transfer coefficient

The relationship of heat transfer coefficient of pure water and nanofluids (optimum concentration) with applied heat flux at different inlet subcooling has been shown in Fig. 5.14-5.17. The graphs have been plotted at a mass flux of 12 kg/m^{2}s. In the first part of these graphs, before the surface temperatures reach to the saturation temperature of the fluid, both water and nanofluid are heated by pure forced convection with the mechanism of single phase. With increasing heat flux, the liquid near the wall is superheated and tends to evaporate, forming bubbles wherever there are active nucleation sites. The bubbles transport the latent heat of the phase change and also increase the convective heat transfer by agitating the liquid near the heating surface. The mechanism in this range is called nucleate boiling and is characterized by a very high heat transfer rate for only a small temperature difference. Also, at higher heat fluxes, bubble coalescence and bubble collapsing phenomenon lead the bulk of fluid to be locally agitated. This phenomenon drastically enhances the heat transfer coefficient in the nucleating boiling region. As observed in graphs, at a given mass flux, the variation between water and nanofluids is less for lower heat fluxes in forced convective region for all the three inlet subcooling temperatures with slightly higher values for lower value of subcooling (ΔT_{sub} = 20 K). For water as well as nanofluids, HTC decreases as inlet subcooling increases. However, as applied heat flux increases, HTC variation is larger in case of ΔT_{sub}= 20 K than ΔT_{sub} = 40 K and 60 K in the nucleate boiling region. At 20 K inlet subcooling, evaporative heat flux plays a dominant role over convective heat flux and heat transfer increases due to more number of bubble formation. The nanofluids exhibit significant enhancement in heat transfer coefficient at higher heat flux because of nanoparticle deposition which in turn change the bubble behavior and surface morphology at lower inlet subcooling. Increase in liquid subcooling causes reduction in

evaporative heat transfer and enhancement in condensation around bubbles which are formed on the heater surface. This leads to deterioration of heat transfer at ΔT_{sub}= 40 K and 60 K.

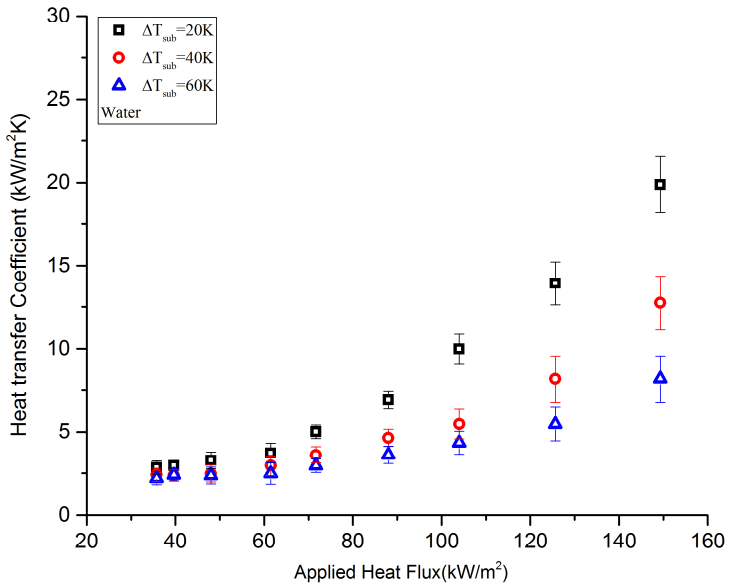

Fig. 5.14 Effect of inlet subcooling on HTC of water

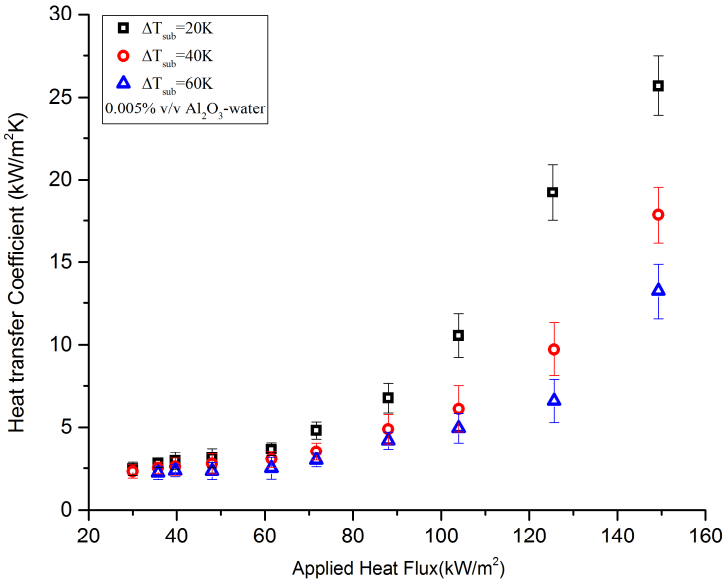

Fig. 5.15 Effect of inlet subcooling on HTC of alumina nanofluid

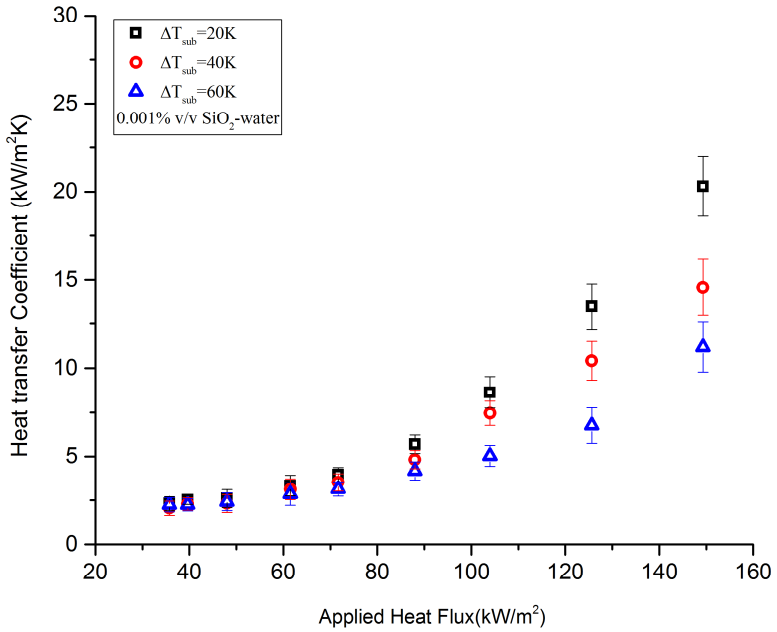

Fig. 5.16 Effect of inlet subcooling on HTC of silica nanofluid

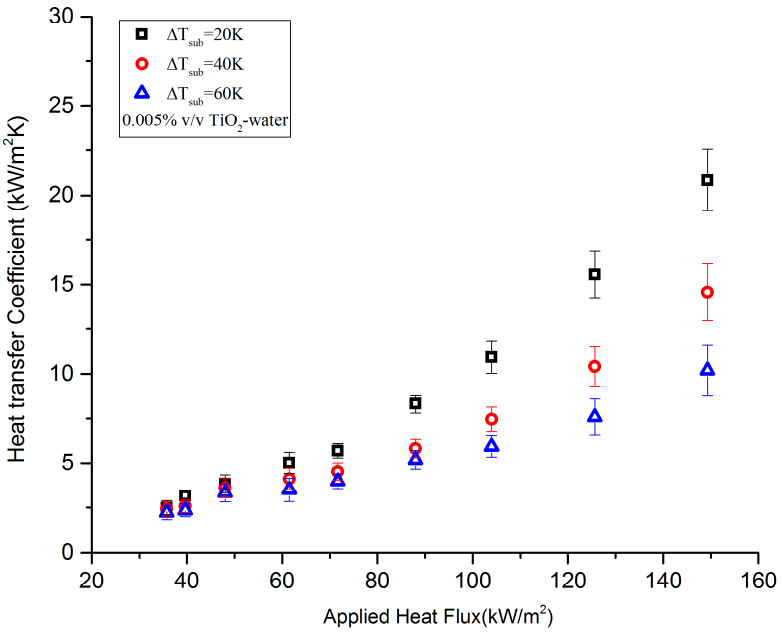

Fig. 5.17 Effect of inlet subcooling on HTC of titania nanofluid

5.5 Delay in DNB

Flow boiling of Al_2O_3-water and TiO_2-water nanofluids (0.001% and 0.01% v/v concentration) have been investigated to study the delay in DNB phenomenon of nanofluids. Experiments have not been conducted till occurrence of DNB as it will damage the heater surface. When highly dense bubbles near the boiling surface is developed, the bubble layer scan block the enthalpy exchange between the wall and bulk flow and trigger a DNB. From the experiments conducted, boiling curves have been plotted and heat transfer coefficients of water and nanofluids have been compared to show the delay in DNB in case of nanofluids.

The boiling curves were obtained by gradually increasing the heat input to the cartridge heater installed in the quartz cylinder until the occurrence of local dry out (The closed symbols in Fig. 5.18-5.21 represent the local dry out condition at which the supply of heat flux is cut off). The outputs from the thermocouples were recorded at 1 s time intervals, and the heat input was controlled manually. Flow boiling curves have been plotted between heat flux and wall superheat on a logarithmic scale with data obtained from experiments conducted for water, Al_2O_3 – water nanofluid, TiO_2 – water nanofluid of volume concentrations 0.001% and 0.01% as shown in Fig. 5.18 and 5.19. The curves show variation of wall superheat as measured by the 2nd thermocouple from the top of the test section. The visual observations were recorded at the same location to validate the results obtained from the temperature-time data (as shown in Fig.6.1). To validate the experimental results, pure water was considered for verification as forced convective and sub-cooled flow boiling heat transfer of water had been investigated by many researchers over a wide range of operating conditions. Exactly similar work with such low flow condition was not available in the literature, however the maximum heat flux of water

which corresponds to local dry out condition of the heater agreed well with the results provided by Kim et al. [141].

During flow boiling experiments using water, small bubbles were observed initially on the heater wall indicating onset of nucleate boiling (ONB). As the heat flux was increased, bubbles coalesced to form larger bubbles which indicated departure from nucleate boiling (DNB). At this point, it was observed that the heater wall was intermittently covered with large vapor bubbles and occasionally with liquid which is the reason for temperature fluctuations as seen in flow boiling curves. Subsequently, churn flow was witnessed with fluid traversing up and down in oscillatory manner with an aggregate upward flow. Churn flow caused the test section to vibrate and also dry patches started to develop on the heater surface in the top part. At this instant, power to the heater was cut-off to avoid burnout of the heater rod.

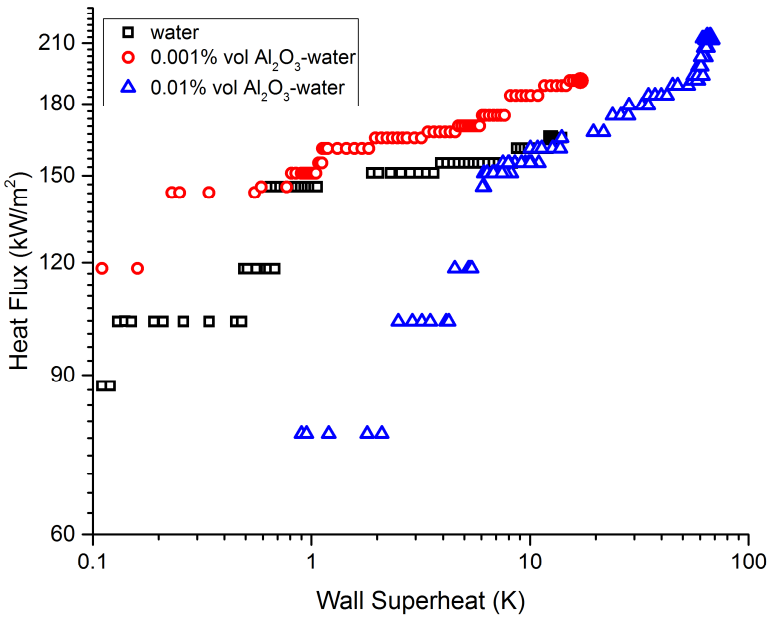

Fig. 5.18. Boiling curves of water and Alumina Nanofluid at the mass flux of 6 kg/m^{2}s.

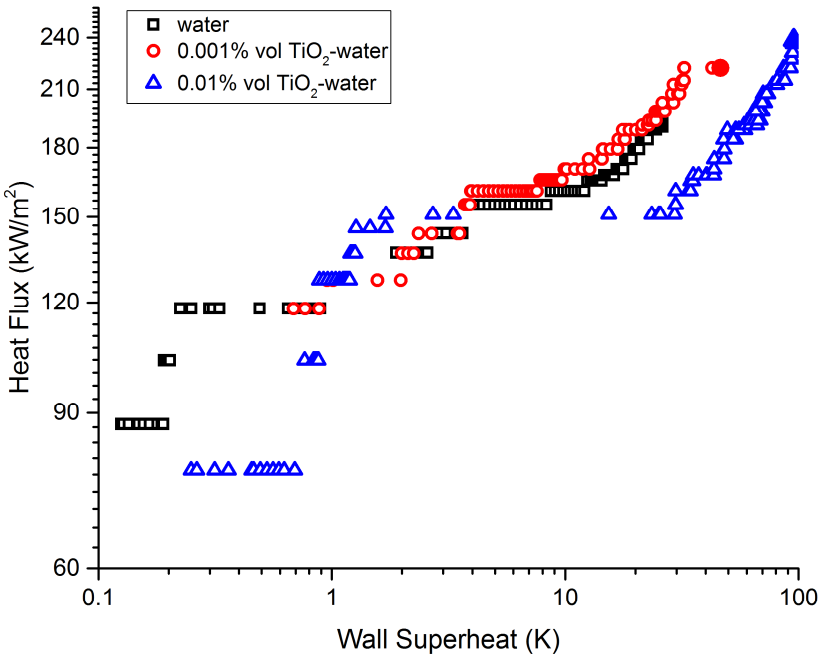

Fig. 5.19. Boiling curves of water and Titania Nanofluid at the mass flux of 6 kg/m^{2}s.

However, during experimentation with Al_2O_3-water and TiO_2-water nanofluids, bubbles do not coalesce easily and discrete bubble regime endures for a longer time even though heat flux was increased. Thus experiments suggest that heater surfaces are continuously modified during nanofluid flow boiling, making nanofluid boiling performance dependent on applied heat flux and particle concentration. It can be observed from the graphs that, in case of both the types of nanofluids, delay in DNB occurred as compared to pure water. With increase in concentration, the nanofluids exhibited very high wall superheat with increasing heat flux.

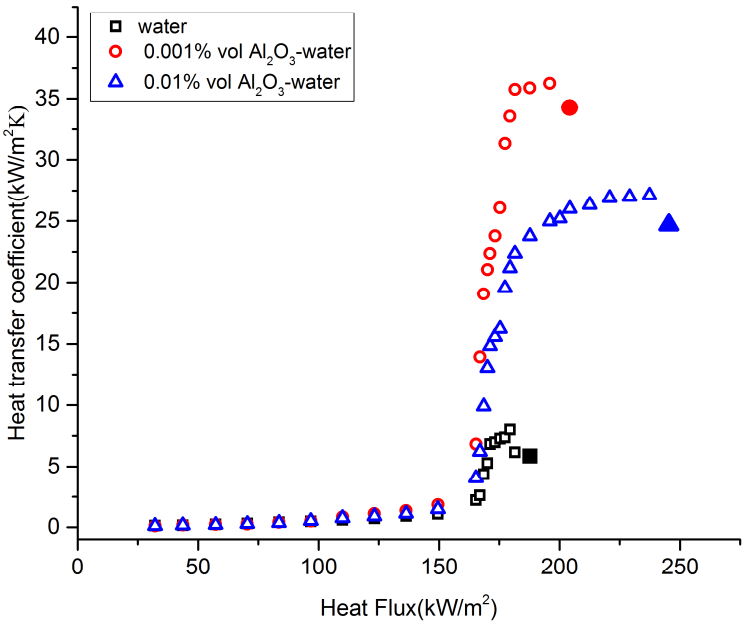

Fig. 5.20. Heat transfer coefficient of water and Alumina nanofluids at 6 kg/m^{2}s.

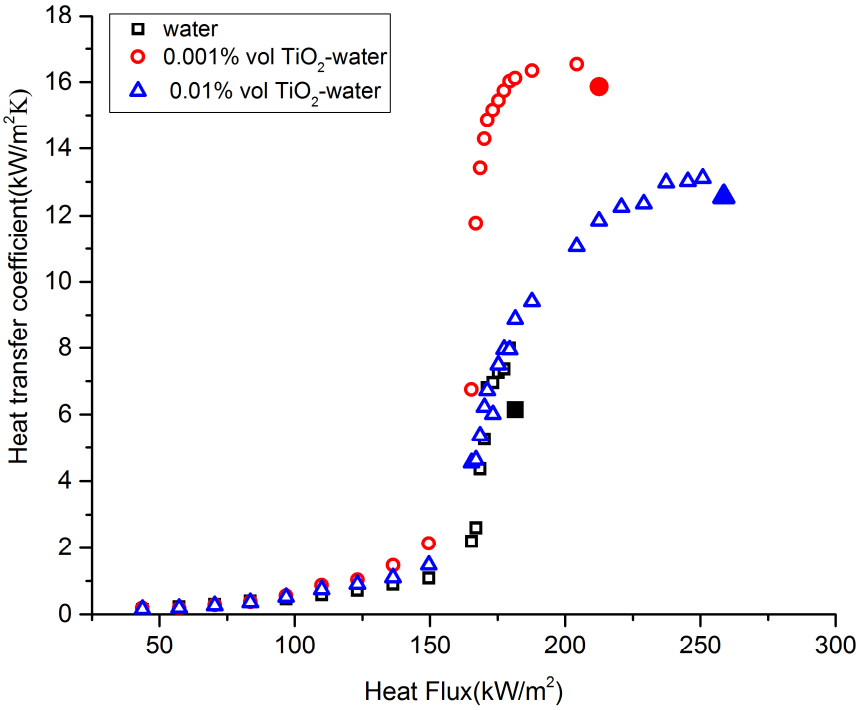

Fig. 5.21. Heat transfer coefficient of water and Titania nanofluids at 6 kg/m^{2}s.

There is a small difference between HTCs of water and nanofluids at relatively lower values of heat flux while the difference enlarges at higher heat flux values as seen in Fig. 5.20 and Fig. 5.21. The graphs exhibit an increasing trend at the beginning indicating forced convection and onset of nucleate boiling (ONB) phenomenon. During nucleate boiling, heat transfer rate is maximum, represented by higher slope which can be seen in the graph. It is observed that heat transfer coefficient is enhanced in case of nanofluid as compared to water, however with increasing concentration, enhancement in heat transfer coefficient decreases. The reason may be attributed to increased thermal resistance caused by excess deposition of nanoparticles on the heater wall at higher concentration of nanofluid during boiling. Delay in DNB, on the other hand is dictated by wetting of the nanoparticle coating generated on the heater surface. As the deposition increases, the wetting of the heater surface increases causing delay in DNB. However, an optimal nanofluid concentration needs to be found out, above which the nanoparticle deposition do not change the wetting characteristics dramatically.

5.5 Summary

In the present investigation, upward flow boiling through a vertical quartz tube has been investigated experimentally using pure water and nanofluids (Al_2O_3-water, TiO_2-water and SiO_2-water) with different concentrations. The effect of supplied heat flux (30-250 kW/m^2), mass flux (3-20 kg/m^{2}s), inlet subcooling (20, 40 °C) and particle volume fraction (0.001%, 0.005% and 0.01% v/v) on heat transfer characteristics have been investigated**.** Results show that, various nanofluids have different optimum volume concentration in which the heat transfer characteristics show the maximum enhancement. The heat transfer coefficient for various nanofluids increases up to optimum volume concentration, and decreases thereafter. In case of nanofluids, DNB has been delayed in comparison to water which was an important observation.